

THE ROUND-ENDED DESIGN AND MEASUREMENT OF ALL SYMMETRIC EDGE-COUPLED BANDPASS FILTER

Bao-Hua Yang^{*}, Ghulam Mehdi, Anyong Hu, Yan Xie, Xian-Xun Yao, Jin Zhang, Cheng Zheng, and Jungang Miao

School of Electronic Information Engineering, Beihang University, Beijing 100191, China

Abstract—The round-corner design of an all symmetric edge-coupled bandpass filter (BPF) is presented. The manufacturing tolerances and its effects of frequency shift on the design of the edge-coupled are investigated. Consequently, the round-ended design method is proposed in order to compensate the open-end effect in the half-wavelength resonator section with the round-ended corners rather than decrementing the lengths in a conventional way, and an experience formula and a corresponding procedure are devised for the design of such filters. The widths of all the half-wavelength resonators are set equal to avoid discontinuities in the interior of the filter. The filter is realized on a ceramic filled soft substrate with dielectric constant of 6.2. For obtaining the de-embedded measured results at the device plane an in-house customized through-reflect-line (TRL) calibration kit is produced. Three kinds of filters at different center frequencies are manufactured, and their measured results are in good agreement with the simulated ones after calibration.

1. INTRODUCTION

The human security inspection has become the common focus of many governments. Its security, humanization and efficiency are raised with high requirement [1, 2]. The conventional X ray human security inspection system may have some harm. As millimeter wave (MMW) electronic technologies have matured, the passive MMW imaging used for human bodies security inspection is emerging as an effective approach to imaging through obscuring materials, such as clothing for

Received 26 January 2013, Accepted 25 March 2013, Scheduled 29 March 2013

^{*} Corresponding author: Bao-Hua Yang (yangbaohua728@163.com).

concealed weapons detection or plastic mines with no harm for human body. Various passive MMW imaging systems have been reported [3–8].

The passive MMW imaging technology has high-level compact integration and resolution. The front-ends of their MMW receiver are realized using MMICs while the passive components, such as filters, are often realized off-chip [9]. The bandpass filters are used in the radio frequency receivers for suppression of the image frequency which results in improved noise figure, especially for parallel coupled microstrip lines filter which has many advantages, such as easy design procedure, wide bandwidth, planar structure, long-narrow aspect ratio and the ability to be placed axially rotated in the receiver channel [9, 10]. However, the filter is sensitive to the spacing between the resonator strips and its length, particularly in the first stage quarter wave coupling section on either side [11].

In this work, a round ended corner design procedure is presented, and a solution is brought forward and aimed at the frequency shift caused by etching error. The widths and lengths of the half-wavelength resonators are kept equal to avoid discontinuities [12]. After etching the open ends of coupled line filter resonators become round corner, and their open-end have capacitors effects. In order to compensate the open-end effects the round-ended corners was adopted rather than decrementing the lengths in a conventional way. In order to preset the center frequency, the frequency shift line followed center frequency, and an experience formula was obtained with the designing round-ended corner. The studied tolerance effects and design procedure are discussed in Section 2. The frequency shift line and measured results are described in Section 3 followed by the conclusions.

2. TOLERANCE ANALYSIS

A fabrication tolerance study has been carried out on different fabricated filters. Comparing optical microscope measurement with the layout pattern sent for the fabrication, it is revealed that there is a size reduction from all four sides of the resonator, which is typically 50% of the conductor thickness, and all right angle corners of the resonators are turned into round-ended shapes after the etching. These result in the shift of frequency response of the filter and the worse ripples in the passband.

The design procedure is proposed based on the above mentioned. For the large scale application of filters in passive MMW systems, the accurate characterization of the filter frequency response and the reproducibility of the filters at large scale with repeatable results are

of the primary concern. The substrate filled with ceramic was selected for our application with dielectric constant of 6.2. The procedure and the equations for the design of edge-coupled BPF are reported in the literature [9–11]

$$Z_0 J_1 = \sqrt{\frac{\pi}{2} \frac{\Delta}{2g_1}} \quad (1)$$

$$Z_0 J_n = \frac{\pi \Delta}{2\sqrt{g_{n-1}g_n}} \quad (2)$$

$$Z_0 J_{N+1} = \sqrt{\frac{\pi \Delta}{2g_N g_{N+1}}} \quad (3)$$

$$Z_{0e} = Z_0 [1 + JZ_0 + (JZ_0)^2] \quad (4)$$

$$Z_{0o} = Z_0 [1 - JZ_0 + (JZ_0)^2] \quad (5)$$

where $n = 1, 2, 3, \dots, N + 1$, and $\Delta =$ Fractional bandwidth.

In order to avoid the discontinuities in the interior of the filter, the widths and lengths of all the half-wavelength resonators are set equal, then the frequency response and the ripple of passband are tuned to the design requirement [13–15].

In the coupled filters, the electric fields extend beyond the open end of the line, and the excessive capacitance is produced at the ends. It results in the electrical length of the resonator effectively longer than the nominal length. Then the length of the resonator is typically increased by one third of the substrate thickness, and the desired spectrum of the filter shifts towards lower side. To compensate this effect, a conventional method called pre-short is used, i.e., reducing the length of the line [16, 17]. In this work, the open-end effect is mitigated by making the right angle edges of the resonators to the round-ended corners, and their shapes agree to the condition after etching, as shown in Figs. 1(a), (b) and (c). The frequency shifted toward high side was obtained after EM simulation of four filters at 8 GHz, 12 GHz, 26 GHz and 34 GHz with 12% relative bandwidth. From these results, the frequency shift line with frequency was obtained as in Fig. 2.

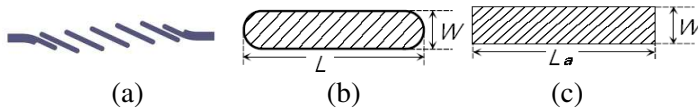


Figure 1. Layout of the edge-coupled BPF after round-ended corner. (a) Filter structure. (b) Round-ended. (c) Equal-area of (b).

From the above figure, the microstrip line width is W . Two right angle edges of the resonator can be converted to the round-ended corners with $\frac{W}{2}$ radius.

Figure 1(c) is the equal-area of (b)

$$L_a = \left(\frac{LW - 2 \left(2 \left(\frac{W}{2} \right)^2 - \frac{\pi}{2} \left(\frac{W}{2} \right)^2 \right)}{LW} \right) L = L - \left(1 - \frac{\pi}{4} \right) W \quad (6)$$

The method that the equal-area of rectangular shape is represented for

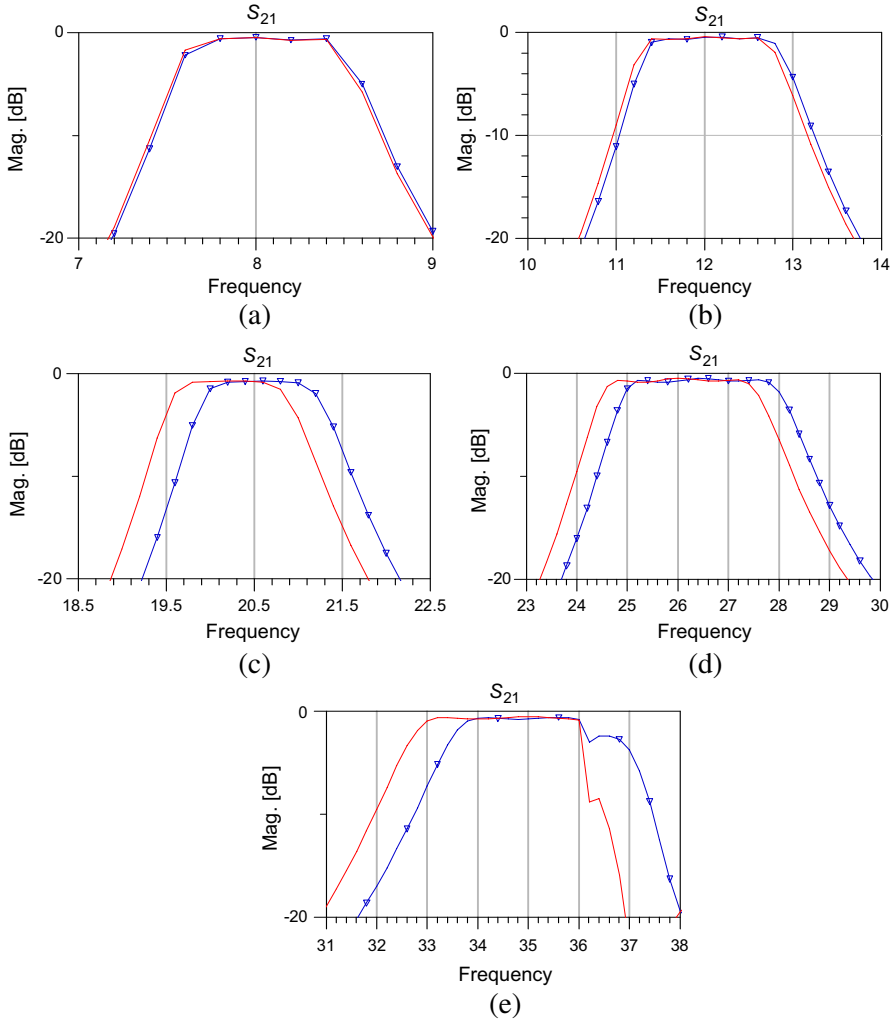


Figure 2. The center frequency shift for $n = 4$.

round-ended shape has been used for antenna [18].

$$\theta = 2\pi \frac{f'_0}{f_0} = 2\pi \frac{L_a}{\lambda_g} \frac{f'_0}{f_0}$$

$$\Delta f_0 = \left(1 - \frac{\theta}{2\pi} \frac{\lambda_g}{L_a}\right) f_0 \quad (7)$$

Eq. (7) shows that the frequency shift is proportional to the center frequency. According to the changed area, the frequency shift is inversely proportional to the stage n of filter.

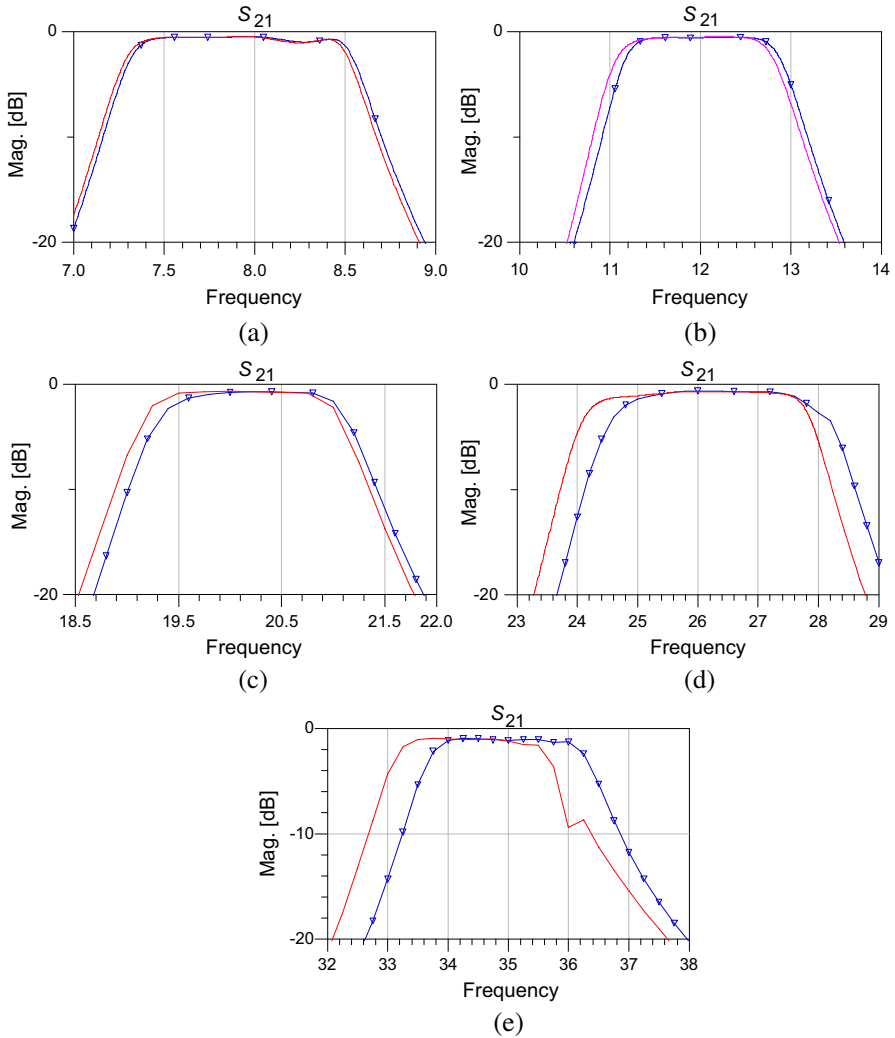


Figure 3. The center frequency shift for $n = 5$.

Based on the etching precision, the gap of the first stage coupled lines is set as 0.1 mm, then the value of width can be obtained. All the widths of the resonator can be equal to those of the first coupled lines, and the only different value of the gap can be obtained. The formula which has been used for calculating w and s is from paper [15].

From Fig. 2 to Fig. 4, the center frequency shifts are shown for $n = 4, 5$ and 6 , respectively whose center frequencies are 8 GHz, 12 GHz, 26 GHz and 34 GHz. The center frequency shifts are tabulated in Table 1.

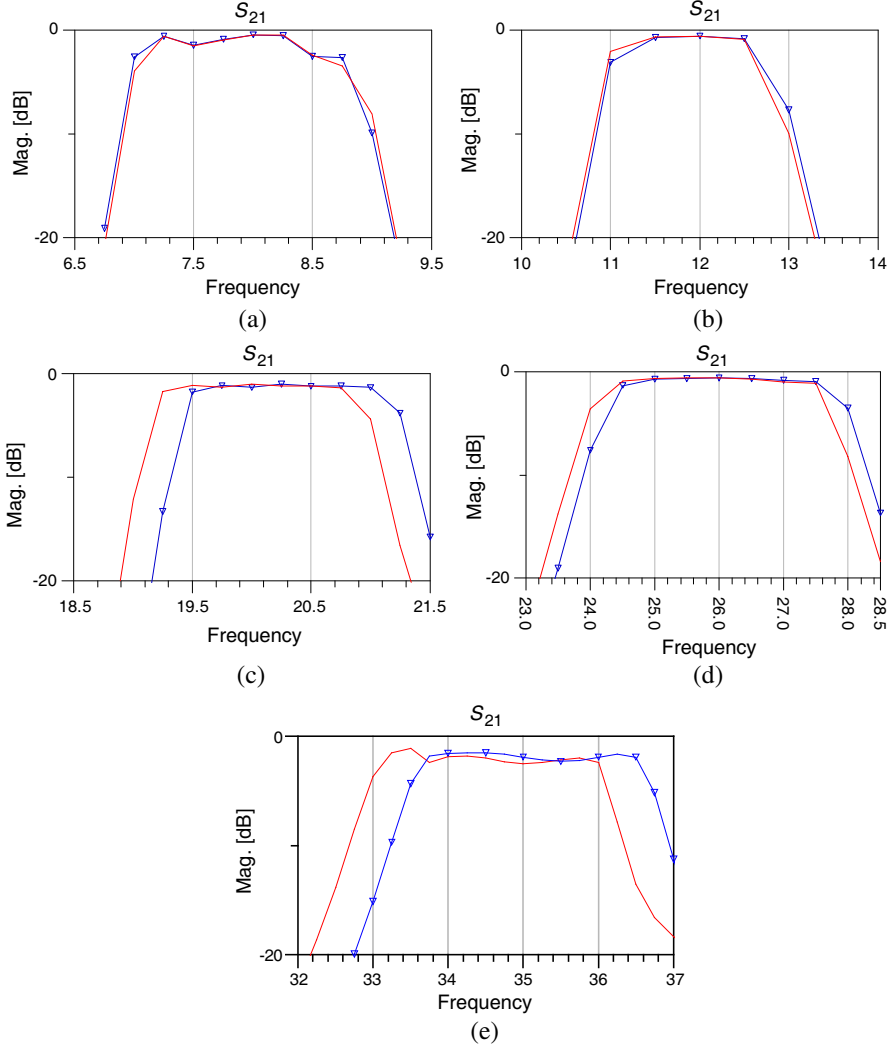


Figure 4. The center frequency shift for $n = 6$.

Table 1. Center frequency shift for different stages.

Center frequency/GHz	Frequency shift/GHz		
	$n = 4$	$n = 5$	$n = 6$
8	0.026	0.024	0.02
12	0.18	0.15	0.045
20	0.39	0.37	0.21
26	0.79	0.45	0.31
34	0.91	0.85	0.57

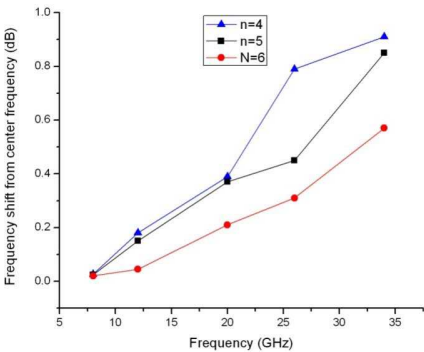


Figure 5. The frequency shift line with frequency.

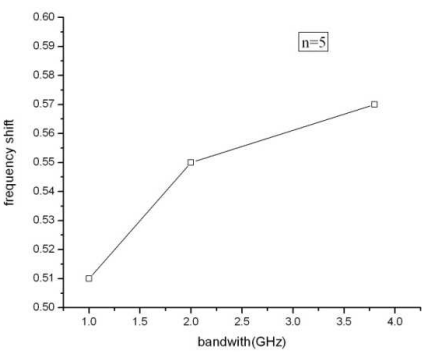


Figure 6. The frequency shift line with relative bandwidth.

Figures 5 and 6 illustrate the frequency shift line with frequency and the frequency shift line with relative bandwidth, respectively. From Fig. 5, an experience formula can be generalized as follow.

$$\Delta f \approx \frac{f_0}{40} \left(\frac{5}{n} \right)^2 \tag{8}$$

From Figure 6, the x axis represents the bandwidth of the 34 GHz filter ranging from 1 GHz to 4 GHz, and the y axis represents the center frequency shift of the 34 GHz filter ranging from 0.51 GHz to 0.57 GHz, so there is no bandwidth item in formula (8). Because the filters are usually used with n values of 4, 5 and 6 at high frequency, only the three kinds of filters are discussed.

Based on formula (8) and the round-ended corner method, the design procedure is obtained for the filter whose resonators have round-ended corner and the same length and width.

- ① The center frequency and bandwidth;

- ② Modify the center frequency according to the formula (8);
- ③ The parameters of prototype lowpass filter according to the filter kind and ripple inter the bandpass;
- ④ Get the other parameters based on the formula (1)–(5);
- ⑤ Get the layout file and change the right-end corner to round-end for the open end of every resonator.

3. MEASUREMENT RESULTS

According to the above procedure, the four kinds of Chebyshev filters are designed at 12.5 GHz, 26.25 GHz and 34.25 GHz with 11.8%, 15.8% and 12% relative bandwidth and 1.5 dB, 0.5 dB and 0.9 dB ripple in bandpass. Their fabricated devices are shown in Fig. 16 which has two 12.5 GHz filters, three 26.25 GHz filters and one 34.25 GHz filter, and (b) is zoomed from (a). The parallel line edge-coupled filter is sensitive to sidewall distance and the top cover height, which is enclosed in a metallic cavity [12]. All test work is carried out in the metallic cavity with 3.8 mm wide and 3.5 mm high for avoiding waveguide dominant mode below 38 GHz. Two sides of the box is connected by K connectors.

Due to the fringing field around the launch region inside the cavity, we get the degraded but symmetric return losses at two ports of the filter. In order to precisely extract the filter response, the Through-Reflect-Line (TRL) calibration kit is produced. By the TRL method [19], the fixture effects are removed from the measured

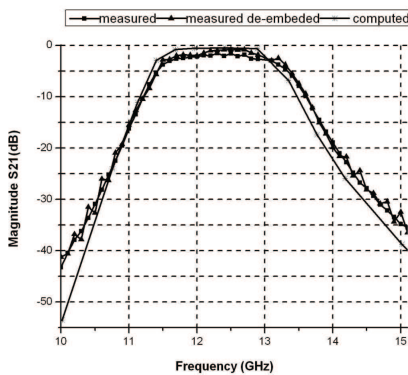


Figure 7. Frequency response of five-pole edge-coupled filter with 12.5 GHz center frequency.

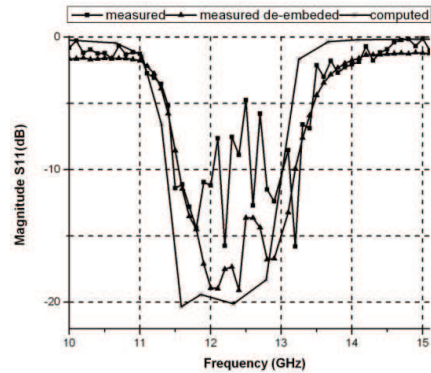


Figure 8. Input return loss of five-pole edge-coupled filter with 12.5 GHz center frequency.

results, called de-embedding. Measurements were carried out at R&S ZVA24. The results are shown in Fig. 7 to Fig. 15. We compared the de-embedded forward transmission response with the embedded and simulated results in Fig. 7, Fig. 10, and Fig. 13. An obvious gap can be seen between the measured filter response and the computed one, which can be reduced after de-embedding. The input and output return losses of the filter are depicted in Fig. 8, Fig. 9, Fig. 11, Fig. 12, Fig. 14, and Fig. 15, respectively. The measured results of some fabricated filters are tabulated in Table 2. The results show excellent match in terms of re-productibility. Differences are observed in de-

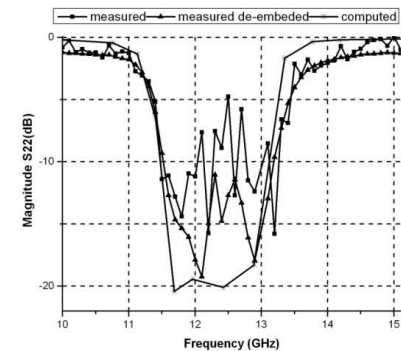


Figure 9. Output return loss of five-pole edge-coupled filter with 12.5 GHz center frequency.

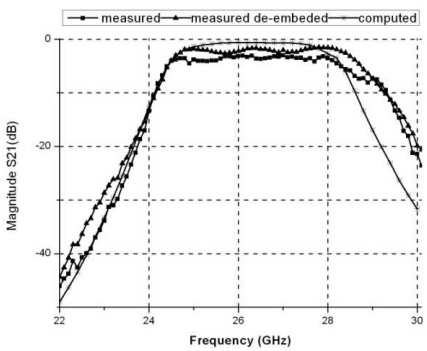


Figure 10. Frequency response of five-pole edge-coupled filter with 26.25 GHz center frequency.

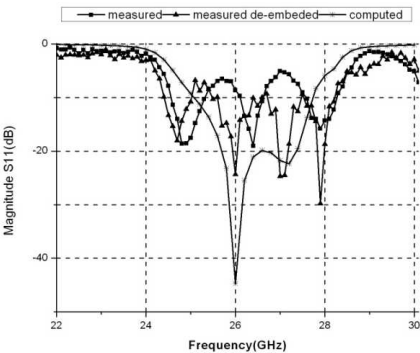


Figure 11. Input return loss of five-pole edge-coupled filter with 26.25 GHz center frequency.

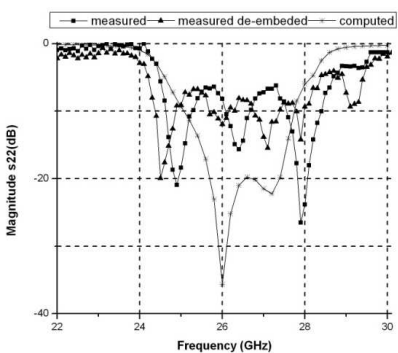


Figure 12. Output return loss of five-pole edge-coupled filter with 26.25 GHz center frequency.

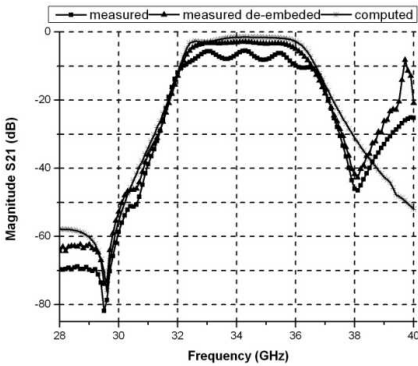


Figure 13. Frequency response of five-pole edge-coupled filter with 34.25 GHz center frequency.

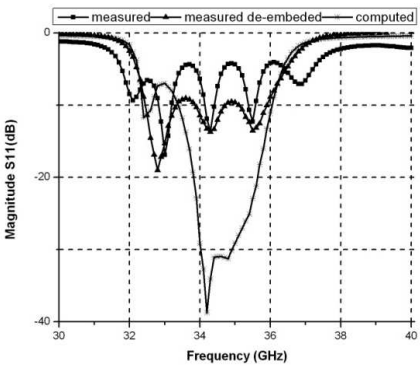


Figure 14. Input return loss of five-pole edge-coupled filter with 34.25 GHz center frequency.

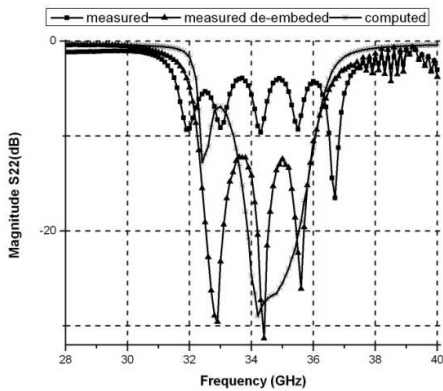
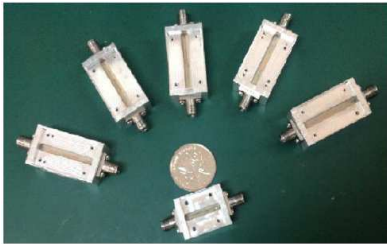


Figure 15. Output return loss of five-pole edge-coupled filter with 34.25 GHz center frequency.



(a)



(b)

Figure 16. Photograph of the fabricated filter, (b) is zoomed from (a).

Table 2. Comparison of fabricated filters.

Parameters	Comparison of two fabricated filters					
	Filter-1	Filter-2	Filter-1	Filter-2	Filter-3	Filter-1
Insertion loss (dB)	1.6	1.7	1.5	1.45	1.51	3
3 dB bandwidth (GHz)	1.48	1.51	4.11	4.14	4.16	3.8
Centre frequency (GHz)	12.5	12.48	26.2	26.23	26.29	34.2
Pass band ripple (dB)	1.5	1.3	0.5	0.54	0.56	0.9
Attenuation at 10 GHz, 22 GHz and 30 GHz (dB)	45	46	46	49	47	55

embedded and computed return losses. Symmetry of the fixtures is mandatory for TRL de-embedding. We attribute these differences to minor asymmetry in the TRL calibration kit. Other possible reason is unwanted coupling from the launch region.

4. CONCLUSIONS

In this paper, the fabrication tolerance effects are studied. A round-ended corner design method based on an experience formula is presented to compensate fabrication tolerances open-end effect. The width of each strip in all coupling sections is set equal to avoid discontinuities inside the filter and accommodate minimum spacing limits. The reduction in length and width of each resonator due to etching process is compensated prior to manufacturing based on our experience formula. Measured results based on TRL calibration method exhibit good agreement with simulated results and validate the design method. The presented method is useful for the design of low loss and high stopband rejection edge-coupled filter.

REFERENCES

1. Liu, S. and H. Jin, "X-ray security inspection technology," *Journal of Security University: Science and Technology*, Vol. 58, No. 4, 78–80, 2008.
2. Sun, L.-N. and P.-X. Yuan, "Research of detection technology in X-ray security inspection equipment," *China Measurement Technology*, Vol. 32, No. 3, 20–23, 2006.
3. Sinclair, G. N., R. N. Anderton, and R. Appleby, "Outdoor passive millimeter wave security screening," *Security Technology 2001 IEEE 35th International Carnahan*, 172–179, Oct. 2001.
4. Anyong, H. and M. Jungang, "Prototype development of an 8mm-band two dimensional interferometer synthetic aperture radiometer," *Proc. IEEE IWISA*, 2009.
5. Wang, N.-N., J.-H. Qiu, and W.-B. Deng, "Development status of millimeter wave imaging systems for concealed detection," *Infrared Technology*, Vol. 31, No. 3, 129–135, China, Mar. 2009.
6. Xue, Y., J. G. Miao, G. L. Wan, A. Y. Hu, and F. Zhao, "Prototype development of an 8 mm band 2-dimensional aperture synthesis radiometer," *2008 International GeoScience and Remote Sensing Symposium*, V-413–V-416, Boston, 2008.
7. Nanzer, J. A. and R. L. Rogers, "Human presence detection using millimetre-wave radiometry," *IEEE Trans. on Microw. Theory & Tech.*, Vol. 55, No. 12, 2727–2733, Dec. 2007.
8. Zheng, C., X. X. Yao, A. Y. Hu, and J. G. Miao, "A passive millimeter-wave imager used fconcealed weapon detection," *Progress In Electromagnetics Research B*, Vol. 46, 279–297, 2013.
9. Cohn, S. B., "Parallel-coupled transmission line resonator filters," *IEEE Trans. on Microwave Theory & Tech.*, Vol. 6, No. 2, 223–231, Apr. 1958.
10. Matthaei, G. L., L. Young, and E. M. T. Jones, *Microwave Filters, Impedance-matching Networks and Coupling Structures*, Artech House, 1980.
11. Gupta, K. C., R. Garg, I. Bahl, and P. Bhartia, *Microstrip Lines and Slotlines*, 2nd Edition, Artech House Inc., 1996.
12. Swanson, D. G. and W. J. R. Hoefer, *Microwave Circuit Modelling Using Electromagnetic Field Simulation*, Artech House Inc., 2003.
13. Feng, L., Z. Wan, and Q. R. Zheng, "An improved genetic algorithm optimizing microstrip filter with equal width," *2003 6th International Symposium on Antennas, Propagation and EM Theory, Proceedings*, 2003.

14. Wang, A.-G. and Q.-N. Lin, "The design for band-pass filter of parallel coupled microstrip lines with equal width," *Journal of Circuits and Systems*, 43–47, 2000.
15. Kirschning, M. and R. H. Jansen, "Accurate wide-range design equations for the frequency-dependent characteristic of parallel coupled microstrip lines," *IEEE Transactions on Microwave Theory and Techniques*, Vol. 32, No. 1, 83–90, Apr. 1984.
16. Mongia, R., I. Bahl, and P. Bhartia, *RF & Microwave Coupled-line Circuits*, Artech House Inc., 1999.
17. Hong, J.-S. and M. J. Lancaster, *Microstrip Filters for RF/Microwave Applications*, John Wiley & Sons Inc., 2001.
18. Liu, D. X., B. Gaucher, and U. Pfeiffer, *Advanced Millimeter-wave Technology*, A John Wiley and Sons, Ltd., Publication, 238–239, 2009.
19. "Agilent in-fixture microstrip device measurement using TRL calibration," Agilent Product Note PN 8720-2, 1991.